Eur. J. Mineral.
2005, **17**, 933–942

Cleusonite, $(Pb,Sr)(U^{4+},U^{6+})(Fe^{2+},Zn)_2(Ti,Fe^{2+},Fe^{3+})_{18}(O,OH)_{38}$, a new mineral species of the crichtonite group from the western Swiss Alps

PIERRE-ALAIN WÜLSER[1,2,4,5]*, NICOLAS MEISSER[1,2], JOËL BRUGGER[4,5], KURT SCHENK[3], STEFAN ANSERMET[1,6], MICHEL BONIN[3] and FRANÇOIS BUSSY[2]

[1]Musée Cantonal de Géologie, CH-1015 Lausanne, Switzerland
[2]Institut de Minéralogie et Géochimie, Université de Lausanne, CH-1015 Lausanne, Switzerland
[3]Laboratoire de Cristallographie 1, EPFL, Dorigny, CH-1015 Lausanne, Switzerland
[4]Cooperative Research Centre for Landscape Environments and Mineral Exploration (CRC-LEME) & School of Earth and Environmental Sciences, The University of Adelaide, North Terrace, Adelaide, AU-5000 Australia
[5]Division of Mineralogy, South Australian Museum, North Terrace, Adelaide, AU-5000 Australia
[6]Musée Cantonal d'Histoire Naturelle de Sion, CH-1950 Sion, Switzerland
*Corresponding author, e-mail: pierre-alain@wulser.com

Abstract: Cleusonite, $(Pb,Sr)(U^{4+},U^{6+})(Fe^{2+},Zn)_2(Ti,Fe^{2+},Fe^{3+})_{18}(O,OH)_{38}$, is a new member of the crichtonite group. It was found at two occurrences in greenschist facies metamorphosed gneissic series of the Mont Fort and Siviez-Mischabel Nappes in Valais, Switzerland (Cleuson and Bella Tolla summit), and named after the type locality. It occurs as black opaque cm-sized tabular crystals with a bright sub-metallic lustre. The crystals consist of multiple rhombohedra and hexagonal prisms that are generally twinned. Measured density is 4.74(4) g/cm^3 and can be corrected to 4.93(12) g/cm^3 for macroscopic swelling due to radiation damage; the calculated density varies from 5.02(6) (untreated) to 5.27(5) (heat-treated crystals); the difference is related to the cell swelling due to the metamictisation. The empirical formula for cleusonite from Cleuson is $(Pb_{0.89}Sr_{0.12})_{\Sigma=1.01}$ $(U^{+4}{}_{0.79}U^{+6}{}_{0.30})_{\Sigma=1.09}$ $(Fe^{+2}{}_{1.91}Zn_{0.09})_{\Sigma=2.00}$ $(Ti_{11.80}Fe^{+2}{}_{3.44}Fe^{+3}{}_{2.33}V^{+5}{}_{0.19}Mn_{0.08}Al_{0.07})_{\Sigma=17.90}$ $[O_{35.37}(OH)_{2.63}]_{\Sigma=38}$. Cations were measured by electron microprobe, the presence of structural (OH) was confirmed by infrared spectroscopy and the U^{6+}/U^{4+} and Fe^{2+}/Fe^{3+} ratios were determined by X-ray photoelectron spectroscopy. Cleusonite is partly metamict, and untreated crystals only show three major X-ray diffraction peaks. Because of this radiation-damaged state, the mineral appears optically isotropic and shows a light-grey to white colour in reflected polarized light. Cleusonite is trigonal, space group $R\bar{3}$, and unit-cell parameters are varying from a = 10.576(3), c = 21.325(5) Å (untreated crystal) to a = 10.4188(6), c = 20.942(1) Å (800°C treatment) and to a = 10.385(2), c = 20.900(7) Å (1000°C treatment). The three cells give a common axial ratio 2.01(1), which is identical to the measured morphological one 2.04(6). The name cleusonite also applies to the previously described "uranium-rich senaite" from Alinci (Macedonia) and the "plumbodavidite" from Huanglongpu (China).

Key-words: cleusonite, new mineral, Swiss Alps, crichtonite group, uranium oxidation state, crystal morphology.

Introduction

The crichtonite group of minerals contains several series of isostructural members, crystallising in the trigonal system with space group $R\bar{3}$, Z = 3 and a unit-cell of a_{hex} ~10.4 Å and c_{hex} ~20.9 Å. They belong to the oxide class 4.CC.40. according to the Strunz classification (Strunz & Nickel, 2001). The crichtonite group presently contains eleven minerals approved by the CNMMN of IMA, including crichtonite *sensu stricto* (De Bournon, 1817; Grey *et al.*, 1976), davidite-(La) and davidite-(Ce) (Gatehouse *et al.*, 1979), loveringite (Gatehouse *et al.*, 1978), mathiasite (Gatehouse *et al.*, 1983), lindsleyite (Zhang *et al.*, 1988), senaite (Grey & Lloyd, 1976), dessauite-(Y) (Orlandi *et al.*, 1997), landauite (Grey & Gatehouse, 1978), gramaccioliite-(Y) (Orlandi *et al.*, 2004) and the new mineral cleusonite (Table 1). Crichtonites are characterised by a common structural formula: $^{XII}A^{VI}B^{VI}C_{18}{}^{IV}T_2(\Phi)_{38}$ (Armbruster & Kunz, 1990; Orlandi *et al.*, 1997), where dominant cations are: ^{XII}A = Ba, K, Pb, Sr, La, Ce, Na, Ca; ^{VI}B = Mn, Y, U, Fe, Zr, Sc; $^{VI}C_{18}$ = Ti, Fe, Cr, Nb, V, Mn, Al; $^{IV}T_2$ = Fe, Mg, Zn; Φ = O, (OH); cations known to dominate in natural samples are underlined. This formula reflects the great variability for the compositions of the mineral. However, only Ti, Fe and O are systematically present. Ti (^{VI}C) accounts for 10 to 16 apfu in all hitherto analysed crichtonites. The nomenclature of the group is based upon the combination of dominant cations in the sites ^{XII}A and ^{VI}B (Orlandi *et al.*, 1997). The crystal structure is

DOI: 10.1127/0935-1221/2005/0017-0933
0935-1221/05/0017-0933 $ 4.50

Table 1. Structural formula of the crichtonite group members.

	Revised simplified formula ($^{XII}A^{VI}B^{VI}C_{18}{}^{IV}T_2(\Phi)_{38}$)					Key references
	M0 (A)	M1 (B)	M2 (T)	M3-4-5 (C)	Φ	
Landauite	Na,Pb	Mn,Y	Zn_2	Ti,Fe,Nb	O,OH	Grey *et al.* (1978)
Loveringite	Ca,LREE	Zr,Fe	$(Mg,Fe)_2$	Ti,Fe,Cr,Al	O	Gatehouse *et al.* (1978)
Lindsleyite	Ba,K	Zr,Fe	$(Mg,Fe)_2$	Ti,Cr,Fe	O	Zhang *et al.* (1988)
Mathiasite	K,Ba,Sr	Zr,Fe	$(Mg,Fe)_2$	Ti,Cr,Fe	O	Gatehouse *et al.* (1983)
Davidite-(La)	La,Ce,Ca	Y,HREE,U	$(Fe,Mg)_2$	Ti,Fe,Cr,V	O,OH	Gatehouse *et al.* (1979)
Davidite-(Ce)	Ce,La	Y,HREE,U	$(Fe,Mg)_2$	Ti,Fe,Cr,V	O,OH	*Idem*
Crichtonite	Sr,Ba,Pb	Mn	$(Fe,Zn)_2$	Ti,Fe	O	Grey *et al.* (1976)
Dessauite-(Y)	Sr,Pb	Y,U	$(Fe,Zn)_2$	Ti,Fe	O	Orlandi *et al.* (1997)
Senaite	Pb,Sr	Mn	$(Fe,Zn)_2$	Ti,Fe	O,OH	Grey *et al.* (1976)
Gramaccioliite-(Y)	Pb,Sr	Y,Mn	$(Fe,Zn)_2$	Ti,Fe	O	Orlandi *et al.* (2004)
Cleusonite	Pb,Sr	U	$(Fe,Zn)_2$	Ti,Fe	O,OH	*This paper*

Notes: Simplified formula of the crichtonite group have been reviewed by a compilation of the published analyses, using the classification scheme given by Orlandi *et al*. (1997). The formulae show the elements that are characteristic of the natural species, for example small amount of Nb for landauite; Zn for Pb/Sr crichtonite end-members. Additional cations on octahedral sites (Armbruster & Kunz, 1990; Orlandi *et al.,* 1997; Gatehouse *et al.,* 1983) are not considered here

based on a close-packed anion framework with a nine-layer stacking sequence (*hhc hhc hhc*) in which ^{XII}A occupies one of the anion sites within the cubic layers. The other metals occupy 18.0 at. % of the octahedral and tetrahedral interstices (^{VI}B, $^{VI}C_{18}$ and $^{IV}T_2$). This occupancy is lower than in the common Ti-Fe oxides (22.2 at. % for ilmenite, 25.0 at. % for magnetite). Crichtonites can contain hydroxyl groups. Hence, it is not possible to calculate Fe^{2+}/Fe^{3+} ratios in crichtonites reliably from electron microprobe analyses, and the determination of a correct chemical formula requires independent measurements of the Fe^{2+}/Fe^{3+} ratio and/or hydroxyl content.

The new mineral cleusonite, ideally $(Pb,Sr)(U^{4+},U^{6+})(Fe^{2+},Zn)_2(Ti,Fe^{2+},Fe^{3+})_{18}(O,OH)_{38}$, was found in the Cleuson valley, in the upper Val de Nendaz (Valais, Switzerland) and named after its location. A second occurrence of cleusonite was subsequently discovered close to the Bella Tolla summit (St-Luc, Val d'Anniviers, Valais), 35 km away from the original find. The new mineral and its name have been approved by the IMA "Commission on New Minerals and Mineral Names" (IMA 1998-070). Holotype crystals (all from Cleuson) are stored in the collections of the Geological Museum of Lausanne, Switzerland (MGL #65200 to 65205). Several cotypes have been deposited in the National Museum of Natural History of Paris, France (MNHNP #203.64 to 203.66). All the reference data have been acquired on holotype crystals of the type locality.

For many years, uranium-bearing crichtonites have been described by a number of names, such as "miromirite" (Damjanovic & Vukasovic, 1961), "plumbodavidite" (Wang, 1981), "uraniferous davidite" (Meixner, 1979), "uraniferous senaite" (Armbruster & Kunz, 1990) and "romanite" (Dragila, 1990). The cleusonite end-member fills an important gap in the nomenclature of the U-bearing crichtonite-group minerals.

Occurrences

Crichtonite-group of minerals occur at several localities in the metamorphosed rocks of the central Swiss Alps (Fig. 1). Cleusonite was found in June 1995 by one of the authors (P.-A. W.) while revisiting radiometric anomalies reported during previous scintillometric surveys (Schaer, 1959) in the Cleuson area (Wülser, 1996); the mineralisation containing cleusonite is hosted by an Alpine (*i.e.* Oligocene-Miocene in age) quartz-chlorite-sulphides bearing vein (Fig. 2) crosscutting a Permian volcanosedimentary series consisting of gneiss with metaconglomerates, metapelites and metarhyolitic lava flows in stratiform position. This series belongs to the Mont Fort Nappe in the Penninic domain of Valais (Thélin *et al.*, 1993; Wülser, 2002) and was metamorphosed under greenschist facies during Alpine orogenesis. The vein paragenesis includes quartz, chlorite, calcite, albite, microcline, "tourmaline", fluorapatite, zircon, ilmenite, hematite, titanite, pyrite, chalcopyrite, tennantite (containing inclusions of tiemannite and hessite), rutile, Nb-bearing rutile, crichtonite, cleusonite, monazite-(Ce), and native gold. Clausthalite, chalcopyrite and uraninite have been found as inclusions (up to 30 μm) in cleusonite. Secondary minerals include copper hydroxy-sulfates and iron hydroxides; no secondary uranium-bearing minerals have been found. Cleusonite appears as single or twinned crystals up to 2–3 cm in diameter (Fig. 3). Minute crystals are also disseminated in the chlorite-rich pods between quartz masses and less frequently sit on the quartz. The chloritic gneiss hosting the vein contains sulphides but no cleusonite. Cleusonite is often rimmed by tennantite and secondary copper minerals when disseminated in the chlorite.

A second occurrence of cleusonite was discovered in 2003 by one of the authors (S. A.) during revisiting a radioactive anomaly of the same type located close to the Bella Tolla summit (3025 m), only 29 km away from the first occurrence (Fig. 1, pt 4). The mineralisation occurs in the Precambrian polymetamorphic (Variscan and Alpine) gneissic basement of the Siviez-Mischabel Nappe, which belongs to the same paleogeographic Penninic domain as the Mont Fort Nappe, but is a structurally lower unit (Thélin *et al.*, 1993). The mineralisation is located several metres away from the discordant contact with Triassic series (quartzites and arkoses) forming the Bella Tolla summit. Cleusonite oc-

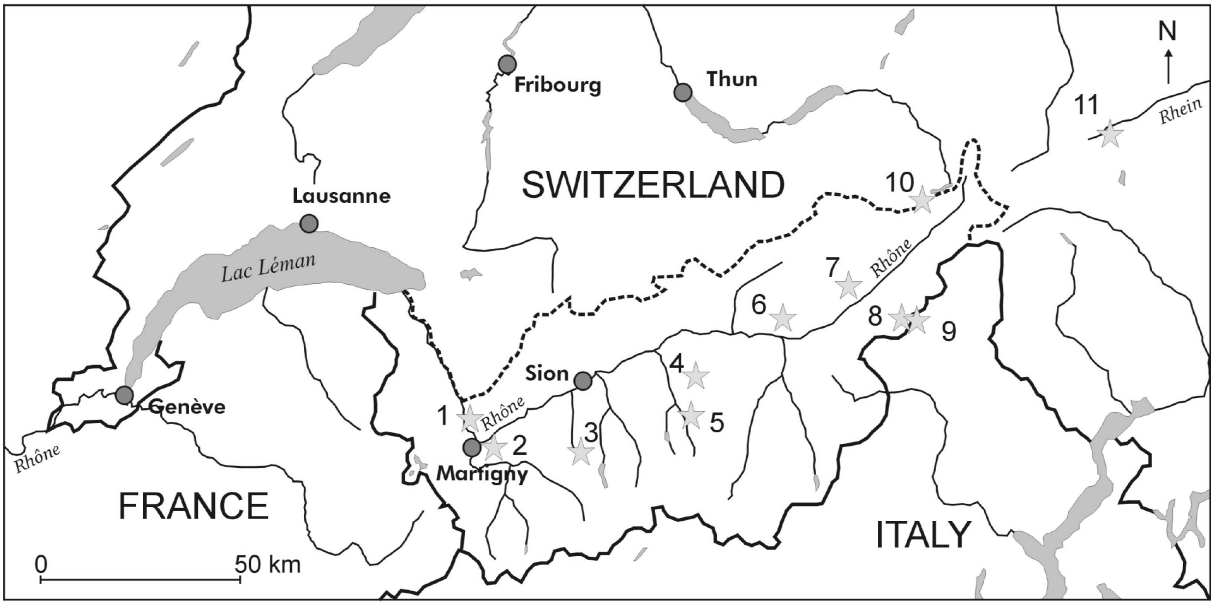

1. Les Plex, Collonges (VS)
2. Tête des Econduits, Chemin (VS)
3. Cleuson, Nendaz (VS)
4. Bella Tolla, Chandolin (VS)
5. Mine des Bourimonts, Ayer (VS)
6. Gärsthorn, Visp (VS)
7. Steinbruchgraben, Raaft (VS)
8. Wannihorn area, Binn (VS)
9. Pizzo Cervandone area, Devero, (I), Binn (VS)
10. Oberaar, Grimsel (BE)
11. Selva, Tavetsch (GR)

Fig. 1. Occurrences of crichtonites in Swiss Alps.

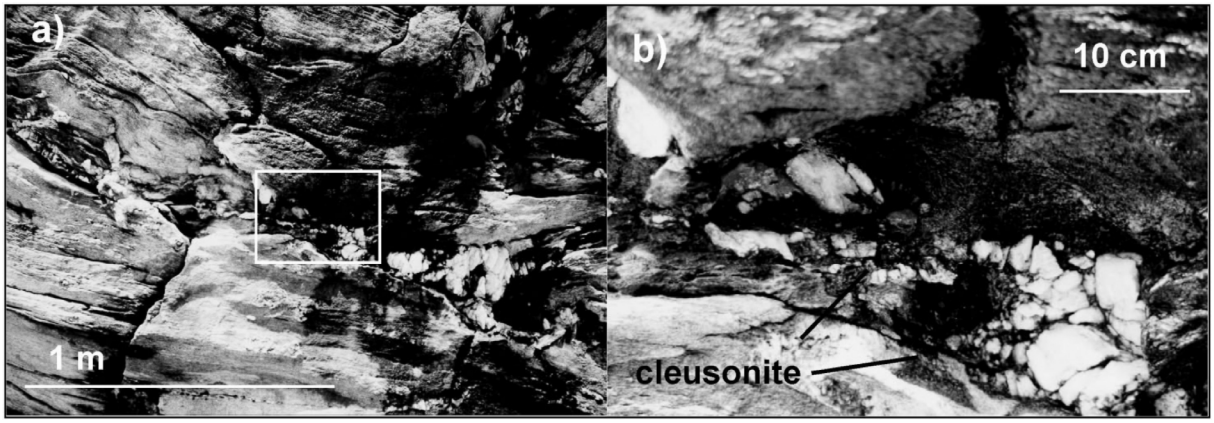

Fig. 2. Cleusonite-bearing Alpine vein at Cleuson: a) vein; b) detail on cleusonite crystals.

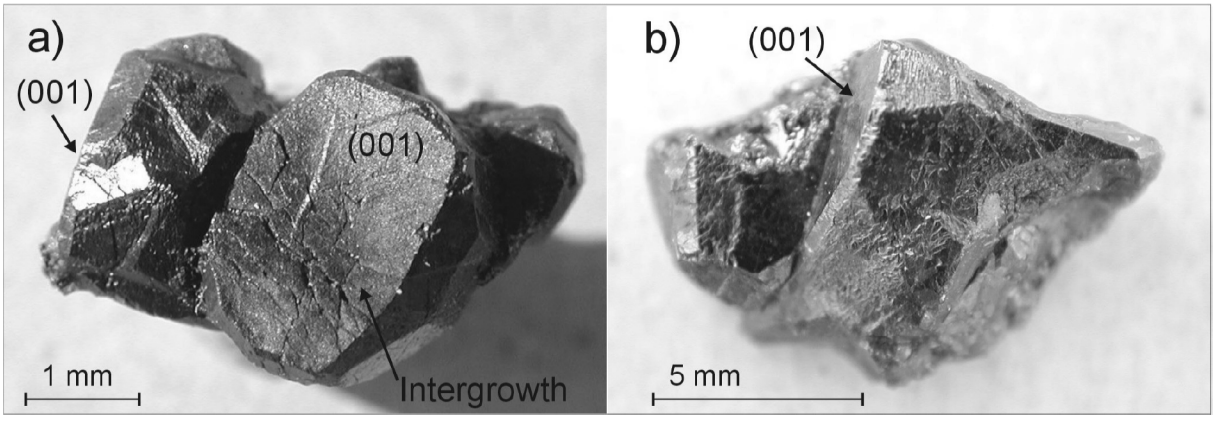

Fig. 3. Cleusonite crystals: a) multiple twinned prims; b) twin used for morphological measurements.

Table 2. Reflectance values in air.

Λ[nm]	400	420	440	460	480	500	520	540	560	580	600	620	640	660	680	700
R [%]	21.2	20.1	19.1	18.4	18.3	17.9	17.7	17.5	17.3	17.4	17.3	17.4	17.4	17.3	17.1	17.3

Notes: Measurements in air. Silicium carbide (SiC) used as standard

curs as disseminated, flattened masses along the schistosity of the gneiss, as well as in crosscutting Alpine quartz veins. The paragenesis includes quartz, albite and barytine, disseminated chalcopyrite, massive uraninite, Hg-bearing tennantite, pyrite, hematite and magnetite. Secondary minerals are mainly malachite and earthy cinnabar. Orange crystalline crusts of billiétite develop on uraninite. Cleusonite and uraninite are systematically surrounded by red cryptocrystalline hematitised rings produced by the oxydation of Fe^{2+} by the α-decays of uranium series ($He^{2+} + 2Fe^{2+} = He(g) + 2Fe^{3+}$).

Physical and optical properties

Cleusonite crystals are black, opaque with black streak and sub-metallic lustre. Mohs' hardness is 6 to 7. Cleavage was not observed; crystals are brittle and fracture is conchoidal. The colour in polarised reflected light is light-grey to white. No internal reflections have been observed. Because of its partly metamict state, cleusonite appears optically isotropic and neither bireflectance nor pleochroism have been observed. Reflectance measurements are given in Table 2. Values are similar to those of other members of the crichtonite group. Cleusonite is paramagnetic and can be separated using electro-magnets. Values for Frantz Isodynamic Separator are in the range of 0.25 to 0.30 Å, side tilt 15°, forward tilt 25°, for grain sizes between 100 μm and 1 mm. The density measured by immersion in heavy liquid on 17 g of crystals is 4.74(4) g/cm^3.

Metamictisation

Cleusonite is radioactive due to its uranium content. Crystals of cleusonite are always fractured (Fig. 4). A statistical evaluation of the characteristics of the cracks (average spacing and width) allows an estimate of the empty volume in the mineral. The mean spacing is 114 ± 5 μm and the mean width is 1.5 ± 0.5 μm (n = 55). The volume represented by cracks is hence around 4 ± 2 %, corresponding to a swelling of 1.04(2). This expansion is characteristic of radioactive minerals that are undergoing metamict transformation (Graeser & Guggenheim, 1990). This macroscopic swelling produces radial fractures around cleusonite, which are especially visible when cleusonite is included in quartz, and it has been observed in both occurrences. The measured density of 4.74(4) g/cm^3 is related to the fissured crystals and can be corrected to 4.93(12) g/cm^3 using the swelling coefficient (Fig. 5). The calculated densities (X-ray diffraction) range from 5.02(6) g/cm^3 for untreated crystals to 5.27(5) g/cm^3 for heat-treated crystals (Table 6). This difference is explained by the crystallographical swelling of the original unit-cell (V = 1952 Å^3) to a larger radiation-damaged cell (2066 Å^3) as described for the zircon cell (Salje *et al.*, 1999). The resulting swelling is 5.8 %, in addition to the mean macroscopic swelling (~ 4 %).

Goniometric study of crystal morphology

Previous goniometrical studies on crichtonites are available in literature (Bannister & Horne, 1950; De Bournon, 1817; Hey *et al.*, 1969; Il'menev *et al.*, 1972; Oberholzer *et al.*, 1997). These studies often report a steep rhombohedron σ = ~67°; σ representing the dipping angle between the basal plane and the measured face. Oberholzer *et al.* (1997) determined the axial ratio *c*/*a* = 2.05, using the (102) faces of a prismatic crystal of senaite (σ = 67.1°).

The goniometrical study of cleusonite has been conducted on a HUBER two-circle goniometer. About fifteen crystals or twins were studied and a well-developed short prismatic crystal with numerous faces has been chosen for the calculation of the axial ratio (Fig. 3b). An X-ray "powder" diffraction pattern was obtained from the (001) basal faces of two other single prismatic crystals to confirm the structural orientation of the prisms (see X-ray diffraction). The following forms are observed: basal pinacoid, hexagonal prisms and rhombohedra. An idealized view of the measured crystal is shown in Fig. 6. The symmetry corresponds to the $\overline{3}$ point group. Crystals are generally twinned; the twinning being especially well developed on planes parallel to the c-axis (Fig. 3a). Some crystals show interpenetration twins with c as the twin axis; the twins are rotated by ~30° relative to each other about this axis, resulting in an apparent dihexagonal prism. Entering angles permit to recognise this

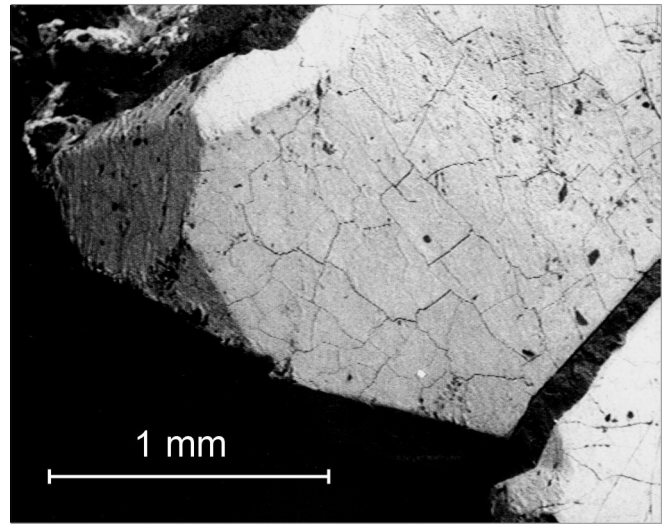

Fig. 4. Back-scattered SEM image of the surface of a cleusonite crystal, showing cracks indicative of macroscopic swelling caused by metamictisation.

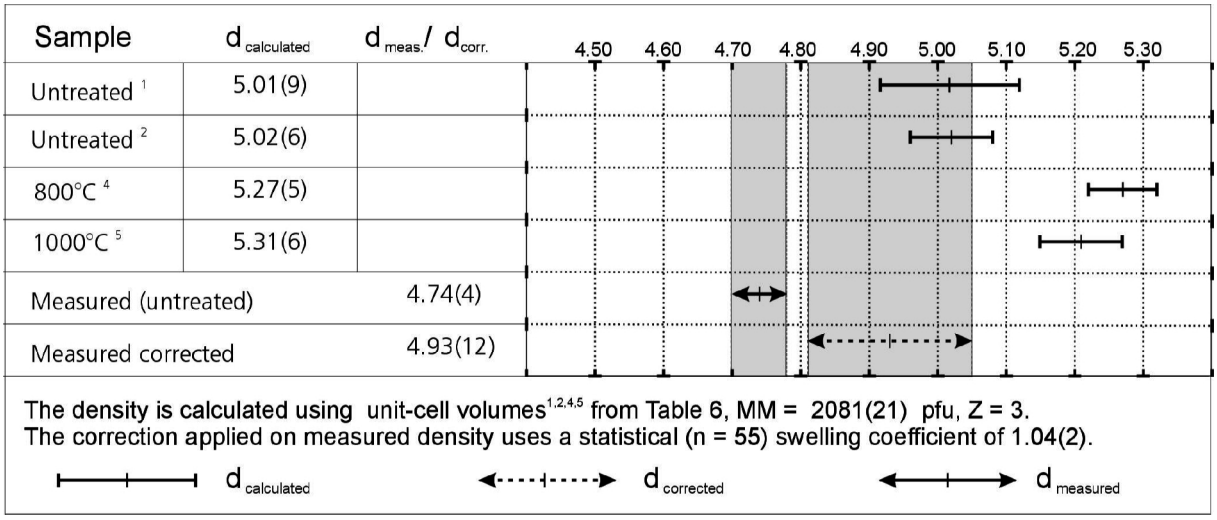

Fig. 5. Density measurements and calculations.

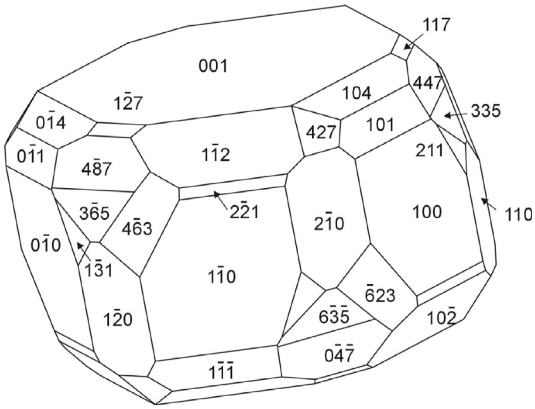

Fig. 6. Ideal representation of the morphology of the cleusonite crystals from goniometrical measurements.

twinning. In addition, the rhombohedra (447) and (101) give a perfect illusion of a trigonal scalenohedron, because of their very close σ angles (66.99° and 67.20°), which are undistinguishable in the incertitude of the measurements. Both the dihexagonal prism and the trigonal scalenohedron correspond to the symmetry of the $\bar{3}2/m$ point group, giving an impression of symmetry higher than $\bar{3}$. Most of the rhomboedra do not appear fully on single crystals. The measured morphological *c/a* axial ratio of cleusonite is 2.04(6) (Table 3).

Chemical data

The chemical composition of cleusonite was obtained by means of electron microprobe analysis (EMPA), X-ray photoelectron spectroscopy (XPS), photo-acoustic Fourier Transform infrared spectroscopy (PA-FTIR), thermogravi-

Table 3. Goniometrical measurements on the large individual crystal of the twin MGL #65203 (see Fig. 3b).

Meas. φ [°]	meas. σ [°]	[1](hkl)	calc. σ [°]	Form
		c/a : 2.04(6)		
–	0.00 ± 0.20	(001)	–	Pinacoid {001}
77.62 ± 0.70	30.54 ± 0.30	(0-14)	30.74	Rhombohedron {104}
289.76 ± 0.95	30.60 ± 0.50	(117)	30.48	Rhombohedron {117}
349.99 ± 0.20	49.46 ± 0.20	(4-27)	49.65	Rhombohedron {4-27}
18.56 ± 0.40	50.53 ± 0.55	(1-12)	49.94	Rhombohedron {012}
289.70 ± 0.45	66.85 ± 0.20	(447)	66.99	Rhombohedron {447}
77.48 ± 0.60	67.09 ± 0.25	(0-11)	67.20	Rhombohedron {101}
49.75 ± 0.35	68.76 ± 0.20	(3-65)	67.98	Rhombohedron {335}
32.73 ± 0.20	75.80 ± 0.25	(4-63)	76.59	Rhombohedron {4-63}
18.36 ± 1.00	78.30 ± 2.00	(2-21)	78.13	Rhombohedron {211}
308.70 ± 1.20	80.50 ± 0.20	(211)	80.97	Rhombohedron {211}
320.23 ± 0.35	89.49 ± 0.83	(100)	–	Hexagonal prism {100}
48.48 ± 0.20	90.16 ± 0.50	(1-20)	–	Hexagonal prism {110}
21.27 ± 0.60	90.41 ± 0.70	(1-10)	–	Hexagonal prism {100}
349.25 ± 0.20	112.91 ± 0.20	(6-3-5)	112.02	Rhombohedron {335}
17.50 ± 0.20	113.00 ± 0.20	(1-1-1)	112.80	Rhombohedron {101}

[1](hkl) based on the crichtonite cell model; *c/a* ratio has been obtained by statistics on the *c/a* of each measured face. φ is the planar orientation; σ is the dipping angle

metric analysis (TGA) and wet spectrocolorimetry. XPS was used to determine oxidation states of Fe, U, Ti, Pb, and Fe^{2+} was also analysed using spectrocolorimetrical wet chemical analysis. PA-FTIR data were used for qualitative detection of hydroxyl and TGA to confirm the absence of weakly bound molecular water.

EMPA was carried out on a CAMECA SX-50 electron microprobe at the Institute of Mineralogy and Geochemistry of the University of Lausanne. Hundreds of analyses have been carried out and the homogeneity was verified along several profiles across four different crystals (polished section MGL #65200). The analytical conditions were 20 kV, 30 nA, spot size 1 µm; the following standards were used: synthetic $MnTiO_3$ ($K\alpha$, Mn), hematite ($K\alpha$, Fe), synthetic TiO_2 ($K\alpha$, Ti), crocoite ($M\alpha$, Pb), sphalerite ($K\alpha$, Zn), synthetic Cr_2O_3 ($K\alpha$, Cr), synthetic UO_2 ($M\alpha$, U), synthetic corundum ($K\alpha$, Al), synthetic Y_2O_3 ($L\alpha$, Y), synthetic V_2O_5 ($K\alpha$, V) and synthetic $SrTiO_3$ ($K\alpha$, Sr). Total acquisition time per analysis was 130 s, with 15 s counting time on each peak, except for Y (30 s).

XPS measurements have been made at the Solid State Science Department of the Polytechnical Federal School of Lausanne, using a small spot ESCA PHI 5500, with an Al$K\alpha$ source operated at 12 kV and 250 W. The total acquisition time was 172 s. A large crystal was analysed on a freshly polished surface of 1 x 3 mm. Detailed scans were conducted across the cation peaks Pb4*f*, U4*f*, Ti2*p* and Fe2*p*. The U4$f_{7/2}$ peak was fitted with two gaussian/lorentzian peaks with an exponential tail function (Fig. 7). The binding energies were calibrated using the C 1s peak of the adventitious carbon on the surface at 285.0 eV. A good fit is obtained with only U^{4+} and U^{6+}, and hence U^{5+} has not been considered (Finnie *et al.*, 2003). The peak surface, width, shape (gaussian/lorentzian) and asymmetry were allowed to vary. In the final refinement, all the peak shapes were fixed to be gaussian, and the two minor (U^{6+}) peaks were constrained to be symmetric. The percentage of the species is related to the area under the curves (Bancroft *et al.*, 1979). The U^{4+} accounts for 72(3) % of the total U (U4$f_{7/2}$) (Table 4). Empirical errors have been applied using the difference between the two U4*f* lines. The same procedure of deconvolution also shows that Pb is only present as Pb^{2+}, Ti only as Ti^{4+} and Fe^{2+} accounts for 71(3) % of the total Fe. Another quantitative determination of Fe^{2+} was carried out by spectrophotometry using Wilson's modified method (Wilson, 1960): two 50 mg samples were dissolved separately in a H_2SO_4/HF diluted mixture. A solution of NH_4VO_3 in H_2SO_4 is added to prevent oxidation of Fe^{2+}. Solutions were then buffered with H_3BO_3 /CH_3COONa, and Fe^{2+} is complexed with 2,2'-bipyridine; the solutions were measured in the maximum range of absorption of the Fe^{2+} complex at 522 nm with a Metrohm 616 photometer. Fe^{2+} accounts here for 69 % of the total Fe, in agreement with XPS surface data. This confirms that the surface XPS measurements represent the bulk oxidation state. Quantitative Fe^{2+}/Fe^{3+} determinations for crichtonite group minerals are available in the literature and show a dominance of Fe^{2+} for senaite, davidite-(La), davidite-(Ce) and of Fe^{3+} for crichtonite and landauite (Hayton, 1960; Larsen, 1989; Portnov *et al.*, 1966; Smellie *et al.*, 1978).

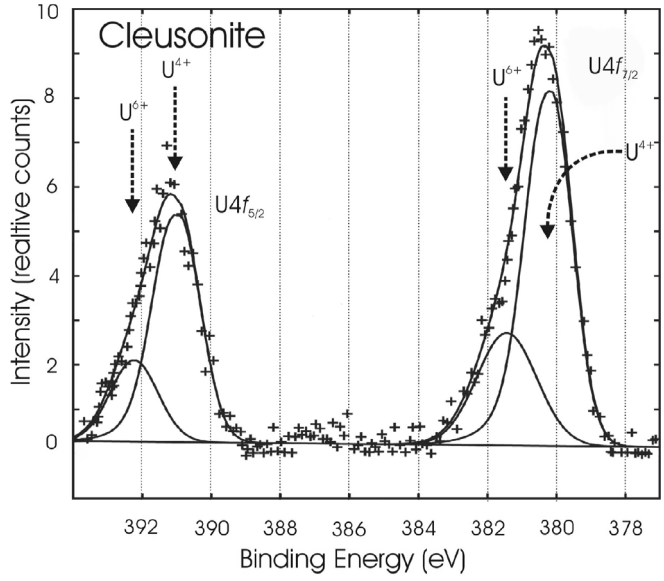

U4$f_{7/2}$: 72 % U^{4+},28 % U^{6+} / U4$f_{5/2}$: 74 % U^{4+},26 % U^{6+}

Fig. 7. Decomposition of the U4$f_{5/2}$ and U4$f_{7/2}$ photoelectron lines.

IR absorption-spectroscopy data were first acquired in the range of 500 to 4000 cm^{-1} on KBr /cleusonite pellets. The transmittance spectrum shows a broad absorption band corresponding to the H-O stretching of the hydroxyl groups at ~3300–3500 cm^{-1} and ~1030–1100 cm^{-1}. However, a minor band at 1650 cm^{-1}corresponding to the H-O-H bending of molecular H_2O could be explained by moisture contamination in the multiple cracks of cleusonite or insufficiently dried KBr.

To clear this ambiguity, a second measurement was undertaken on a 4 mm wide crystal, dried at 60°C during 7 days with silica gel. Half of the crystal was ground up under a nitrogen atmosphere for thermo-gravimetric analysis and introduced into a TGA chamber. The material was heated to 105°C at a rate of 10° per minute (from room temperature) in nitrogen atmosphere. The material was held at 105°C for 60 minutes. TGA showed no weight loss during this time, suggesting no water loss or adsorbed moisture. The second part of the crystal (polished) was then placed in a photoacoustic Fourier Transform Infrared cell (PA-FTIR) (single beam Nicolet Model 750 Magna-IR Spectrometer equipped with an MTEC Model 300 photoacoustic cell assembly) to determine the presence of OH groups. Spectroscopic measurements were run under helium atmosphere; 256 scans were recorded at a resolution of 8 cm^{-1} for a total run time 10 min. (Fig. 8). A broad signal at 3394.14 cm^{-1} indicates the presence of hydrogen bonded OH groups at and below the surface of the sample (up to100 µm of depth). Most of

Table 4. Results of XPS measurement.

	Uranium		Iron	
Envelope	U4$f^{f1/2}$	U4$f^{f1/2}$	Fe2$p^{3/2}$	Fe2$p^{3/2}$
Binding energy (eV)	380.15	381.44	709.58	711.01
Oxidation state	U^{4+}	U^{6+}	Fe^{2+}	Fe^{3+}
% of total area	72(3)	28(3)	71(3)	29(3)

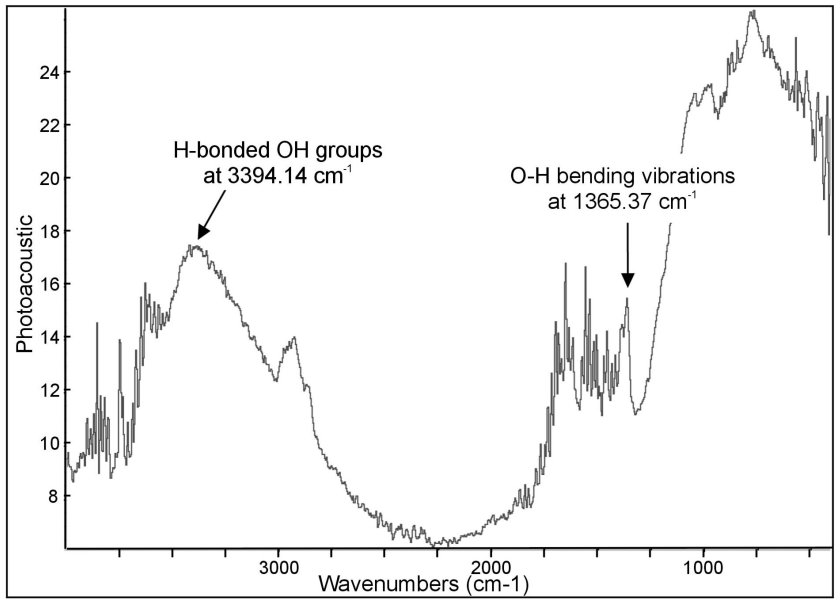

Fig. 8. PA-FTIR spectrum of cleusonite.

such bonded OH groups appear in the 3600–3200 cm^{-1} region of the IR spectrum and the lower the frequency, the stronger the hydrogen bond present (Williams & Fleming, 1980). Free OH groups typically give FTIR signals in the 3700–3600 cm^{-1} range. The signal at 1365.37 cm^{-1} is indicative of O-H bending. PA-FTIR confirms that there are bound OH groups in cleusonite as well as structural H_2O. For comparison, hydroxyl contents of 0.20 weight-% H_2O have been measured in senaite from St. Peters Dome, Colorado (Foord *et al.*, 1984), 0.17 % in the davidite-(La) from Arizona (Pabst, 1961) and 0.68 % in the davidite-(La) from Mavuzi, Mozambique (Smellie *et al.*, 1978).

The final chemical composition (Table 5) integrates a mean of 30 EMPA analyses, spectroscopically determined U^{6+}/U^{4+} and Fe^{3+}/Fe^{2+} ratios and the presence of $(OH)^-$ anions. The $(OH)^-$ content has not been quantitatively determined, but was fixed on the basis of a structural calculation assuming 22 cations and 38 (O,OH). The calculation of an anhydrous formula based on 38 oxygen gives a formula-type of $M_{22.79}O_{38}$. A calculation based on a sum of cations equal to 22 apfu gives a formula of $M_{22}O_{36.69}$. Introducing $(OH)^-$ anions to balance the filling of (O+OH) to 38.00 apfu results in a water content of 1.11 weight-% and an analytical total of 98.33 weight-%. The resulting formula based on the 22 apfu hydroxyled model is: $(Pb_{0.89}Sr_{0.12})_{\Sigma=1.01}$ $(U^{+4}_{0.79}U^{+6}_{0.30})_{\Sigma=1.09}$ $(Fe^{+2}_{1.91}Zn_{0.09})_{\Sigma=2.00}$ $(Ti_{11.80}Fe^{+2}_{3.44}$ $Fe^{+3}_{2.33}V^{+5}_{0.19}Mn_{0.08}Al_{0.07})_{\Sigma=17.90}$ $[O_{35.37}(OH)_{2.63}]_{\Sigma=38}$ with the corresponding molecular mass of 2080.97. Assignment

Table 5. Chemical composition of cleusonite.

oxides	Al_2O_3	TiO_2	V_2O_5	MnO	FeO	Fe_2O_3	ZnO	SrO	PbO	UO_2	UO_3	H_2O	Sum
wt-%	0.16	44.55	0.83	0.28	18.13	8.81	0.33	0.6	9.34	10.07	4.12	1.11	98.33
minimum	0.15	44.08	0.59	0.24	26.66	0.29	0.55	9.01	13.78	–	–		
maximum	0.17	44.82	1.04	0.31	27.25	0.38	0.66	9.60	14.67	–	–		
σ	0.007	0.145	0.110	0.018	0.131	0.020	0.034	0.171	0.165	–	–		
apfu	0.07	11.80	0.19	0.08	5.35	2.33	0.09	0.12	0.89	0.79	0.30	[a]2.63	[b]22.01

simplified formula: $(Pb,Sr)(U^{4+},U^{6+})(Fe^{2+},Zn)_2(Ti,Fe^{2+},Fe^{3+})_{18}(O,OH)_{38}$; [a] (OH); [b] cations sum; MM = 2081.97

Table 6. Unit-cell parameters of cleusonite.

No	Sample	Locality	*a* (Å)	*c* (Å)	V (Å^3)	$d_{calc.}$	Refinement
1	Non-heated powder	Cleuson	10.55(4)	21.42(15)	2065(19)	5.02(10)	UNITCELL on 10 peaks
2	Single crystal	Cleuson	10.576(3)	21.325(5)	2066(2)	5.02(6)	Single cryst. Coll.
3	Single crystal	Cleuson	–	21.24(4)		–	–
4	Heated 800°C in Au foil during18 h	Bella Tolla	10.4188(6)	20.942(1)	1968.7(1)	5.27(5)	Le Bail fit, RIETICA
5	Heated at 1000°C in air during 24 h	Cleuson	10.385(2)	20.900(7)	1952.0(8)	5.31(6)	UNITCELL on 55 peaks

[1] Powder on PW1710 diffractometer, 40 kV, 30 mA, 293K, CuKα, UNITCELL software (Holland *et al.*, 1997)

[2] Single crystal on STOE IPDS imaging plate automatic diffractometer (MoKα, 45 mA, 55 kV, 293K, plate distance: 60 mm, 2θ: 3.8 – 56.3°). 69 images, reflections: 435 > 6σ, 169 > 3σ

[3] Single crystals on PW1820 diffractometer, 40 kV, 40 mA, 293K, CuKα, specific diffraction on (001)

[4] Powder on HUBER diffractometer, imaging plate Guinier camera (670), 35 kV, 34 mA, 293K, CoKα, RIETICA software (Hunter, 1997)

[5] Powder on PW1710 diffractometer, 40 kV, 30 mA, 293K, CuKα, UNITCELL software (Holland *et al.*, 1997)

Table 7. X-ray powder diffraction patterns of heat-treated and untreated crystals.

				Cleuson, heated 1000°C in air – 24 h Rutile peaks suppressed a = 10.385(2), c = 20.900(7) least-square on 55 reflections			Bella Tolla, heated 800°C – in Au foil – 18 h Uraninite peaks suppressed a = 10.4188(6), c = 20.942(1) Le Bail fit on 49 reflections				Cleuson, untreated a = 10.55(4), c = 21.42(15) Least-square on 10 reflections		
No	h	K	l	d(obs)	d(calc)	I/I_0	d(obs)	d(calc)	d(LeBail)	I/I_0	d(obs)	d(calc)	I/I_0
1	0	1	2	6.83	6.82	50.8	6.82	6.84	6.82	42.3			
2	1	1	0	5.18	5.19	51.6	5.19	5.21	5.20				
3	1	0	4	4.51	4.52	15.0	4.52	4.53	4.52	11.3			
4	-2	1	3	4.17	4.16	24.7							
5	2	0	2	4.13	4.13	28.1	4.14	4.14	4.13	47.9	4.19	4.20	4.3
6	0	1	5	3.78	3.79	1.6	3.79	3.80	3.79	1.2			
7	0	0	6	3.480	3.483	30.1	3.480	3.490	3.483	9.2			
8	0	2	4	3.406	3.408	96.4	3.409	3.418	3.409	73.5			
9	2	1	1	3.352	3.355	9.2	3.357	3.366	3.357	3.9			
10	1	2	2	3.230	3.233	39.4	3.234	3.243	3.234	28.7	3.310	3.287	19.0
11	2	0	5	3.064	3.062	46.1	3.062	3.070	3.062	27.9			
12	3	0	0	2.995	2.998	52.5	3.000	3.008	2.999	37.2			
13	1	1	6	2.893	2.893	100.0	2.893	2.900	2.893	100.0	2.957	2.957	16.4
14	2	1	4	2.851	2.849	68.5	2.850	2.858	2.850	57.3			
15	3	0	3	2.752	2.754	26.3	2.756	2.762	2.755	10.0	2.820	2.802	100.0
16	1	2	5	2.635	2.637	23.5	2.638	2.645	2.638	19.7			
17	2	2	0	2.595	2.596	14.2	2.599	2.605	2.598	14.2			
18	0	1	8	2.505	2.509	35.3	2.503	2.514	2.509	5.4	2.567	2.569	11.2
19	1	3	1	2.476	2.477	31.2	2.479	2.485	2.478	21.2			
20	3	1	2	2.426	2.426	24.7	2.430	2.434	2.427	29.9	2.450	2.466	37.9
21	3	0	6	2.272	2.272	6.4	2.273	2.278	2.273	6.9			
22	1	3	4	2.245	2.251	55.1	2.254	2.258	2.252	53.5			
23	0	4	2	2.197	2.198	14.2	2.201	2.205	2.199	2.0			
24	3	1	5	2.141	2.142	21.9	2.144	2.148	2.143	28.4			
25	2	2	6	2.083	2.082	4.0	2.083	2.088	2.082	6.7	2.137	2.122	20.7
26	1	2	8	2.071	2.071	4.5	2.071	2.077	2.072	9.0			
27	4	0	4	2.0643	2.0653	9.8							
28	1	0	10	2.0348	2.0358	4.9	2.039	2.0400	2.0358	5.2	2.081	2.085	14.7
29	2	3	2	2.0231	2.0242	5.0	2.028	2.0307	2.0252	7.9			
30	1	4	0	1.9622	1.9625	12.6	1.965	1.9690	1.9635	13.7			
31	3	2	4	1.9191	1.9190	17.3	1.920	1.9250	1.9199	25.2			
32	0	2	10	1.8955	1.8953	5.2	1.896	1.8995	1.8955	7.9			
33	2	3	5	1.8508	1.8501	7.5	1.853	1.8557	1.8509	7.1			
34	3	1	8	1.8031	1.8041	19.8	1.806	1.8089	1.8046	38.7			
35	2	1	10	1.7805	1.7804	8.5	1.781	1.7846	1.7806	12.0			
36	0	0	12	1.7424	1.7417	2.0							
37	4	1	6	1.7093	1.7098	19.3	1.712	1.7149	1.7105	25.5	1.7406	1.7408	8.6
38	0	5	4	1.7009	1.7008	22.0	1.702	1.7061	1.7015	14.2			
39	3	2	7	1.6982	1.6974	9.0							
40	1	2	11	1.6597	1.6585	2.5							
41	5	0	5	1.6520	1.6522	6.4	1.655	1.6573	1.6529	10.6			
42	2	4	4	1.6175	1.6163	2.8	1.619	1.6213	1.6197	7.6			
43	1	3	10	1.6019	1.6020	22.4	1.604	1.6060	1.6023	47.6			
44	4	2	5	1.5753	1.5744	2.1	1.577	1.5793	1.5751	4.1			
45	3	3	6	1.5495	1.5500	6.0	1.553	1.5547	1.5506	8.8			
46	5	1	4	1.5429	1.5432	4.5	1.546	1.5481	1.5439	7.4			
47	3	1	11	1.5115	1.5115	8.2	1.513	1.5152	1.5117	13.2			
48	4	1	9	1.4995	1.4990	2.0	1.503	1.5031	1.4997	5.3			
49	3	2	10	1.4681	1.4683	1.8							
50	3	4	2	1.4640	1.4639	4.2	1.469	1.4687	1.4687	8.7	1.4850	1.4899	32.8
51	2	5	0	1.4404	1.4401	18.8	1.443	1.4448	1.4408	52.1			
52	4	3	4	1.4231	1.4227	3.8	1.425	1.4272	1.4252	10.0			
53	0	0	15	1.3944	1.3933	2.4							
54	6	0	6	1.3771	1.3769	4.7	1.379	1.3811	1.3774	14.4			
55	1	6	1	1.3681	1.3686	6.4							

Table 8. U- and Pb-rich crichtonites.

Locations	UO_2 %	PbO %	SrO %	Former names	Species
Cleuson, Switzerland	13.96	9.34	0.60		cleusonite
Huanglongpu, China	11.26	8.4	0.58	plumbodavidite	cleusonite
Alinci, Macedonia	10.53	9.76	0.53	uranium-rich senaite	cleusonite
Faraday Mine, Canada	9.30	4.60	0.40	davidite	intermediate davidite-(Ce)/ cleusonite
Pizzo Cervandone, Italy	6.67	4.27	0.22	uranium-rich senaite	intermediate cleusonite / sub-unit
Nezilovo, Macedonia	2.58	11.83	not det.	miromirite	gramaccioliite-(Y) or senaite
Metalliferi Mts, Romania	> 7	5–7	not det.	romanite	cleusonite or new species (if Sr>Pb)

of the cations to the crystallographic sites is in accordance with reported structural formulae of the crichtonite group minerals. The presence of only Fe^{2+} (and minor Zn) instead of Fe^{3+} on the $^{IV}T_2$ site is deduced from the landauite structure (Grey & Gatehouse, 1978), where only Zn^{2+} fills $^{IV}T_2$. U^{6+}, despite of its smaller ionic radius, remains along with U^{4+} in ^{VI}B with a high sum of 1.09 apfu. The simplified structural chemical formula may be written as $(Pb,Sr)(U^{4+},U^{6+})(Fe^{2+},Zn)_2(Ti,Fe^{2+},Fe^{3+})_{18}(O,OH)_{38}$. The corresponding, non-metamict calculated density is 5.14(8) g/cm^3, with an error related to the chemical composition (~ 1 %), errors on the unit-cell volume being insignificant (Fig. 5).

X-ray diffraction

X-ray powder diffraction data were first acquired on untreated crystals which appeared to be in a partly metamict state. Single crystal X-ray diffraction patterns give spots which can be indexed with a hexagonal cell a = 2.933(1), c = 21.325(5) Å. These non-heated sub-cell parameters correspond to the anion closest-packed stacking (O, Pb) and are identical to the ones previously measured on partly metamict loveringite and davidite (Hey *et al.*, 1969; Kelly *et al.*, 1979; Rouse & Peacor, 1968). The X-ray powder diffraction pattern of untreated crystal displays only three major broad peaks (0.4° width at ½-height) and several minor peaks. The cell parameters have been refined using the UNITCELL software (Holland & Redfern, 1997) and give a = 10.55(4), c = 21.42(15) Å. These parameters are similar to those obtained on single crystal: a = 10.576(3), c = 21.325(5) Å (Table 6). An X-ray diffraction pattern was acquired on the basal face of a prismatic non-treated monocrystal; the $(003)^{I=<1\%}$, $(006)^{I=16\%}$, $(009)^{I=100\%}$ and $(0012)^{I=22\%}$ reflections correspond to a c = 21.24(4) Å parameter. These (00ℓ) reflections are too weak to be apparent in the powder X-ray diffraction patterns.

Several heating experiments have been conducted to reconstitute the crystalline state of cleusonite (Tables 6 and 7). A first crystal heated at 1000°C in air during 24 h was refined using UNITCELL and gives a = 10.385(2), c = 20.900(7) Å; an accessory phase (rutile) appears in the diffraction pattern. Another recrystallised crystal (heated at 800°C during 18 h, sealed in gold foil) was refined by a Le Bail fitting using the RIETICA software (Hunter, 1997) and gives the unit-cell parameters a = 10.4188(6), c = 20.942(1) Å.

Review of cleusonite occurrences

Cleusonite, and the recently described gramaccioliite-(Y) end-members, allow to attribute formal names to numerous occurrences of Pb- and U-bearing "crichtonite-group" minerals. A general compilation of previously published crichtonites compositions was necessary to clarify several old denominations (Table 8). The "uranium-rich senaite" from Alinci, Macedonia (Bermanec *et al.*, 1990) and the "plumbodavidite" from Huanglongpu, China (Wang, 1981) are cleusonites, and the old denominations must be abandoned. Some minerals still remain not sufficiently documented to allow a clear denomination: Y not quantitatively analysed for "miromirite" from Nezilovo (Macedonia) (Fleischer, 1973), Sr and Y not analysed for "romanite" from Romania (Dragila, 1990). The uranium-rich senaite from Pizzo Cervandone (Italy) (Armbruster & Kunz, 1990; Stalder & Bühler, 1987) does not match to a clear end-member but is a complicated case of intermediate composition between a Y-bearing cleusonite (<50 %) and a cation deficient sub-unit described in Armbruster *et al.* (1990). The davidite from the Faraday Mine in Canada (Mossman, 1985) represents an intermediate composition between cleusonite (50 %) and davidite-(Ce) (50 %). The crichtonite nomenclature still contains some holes but cleusonite closes an important gap in the nomenclature of uranium-containing crichtonites.

Acknowledgements: The present study was started in 1995, when the first author (P.-A. W.) was undertaking a research for young scientists (Schweizer Jugend Forscht) and had a limited knowledge about new minerals and analytical mineralogy, but the strong will to continue studying that unusual mineral discovery. Many people have helped in that adventure: Dr. B. Tagini, Dr. D. Cavalli, Drs. M. Brianza & N. Brianza, Dr. P. Thélin, L. Nicod, A. Volentik, J.-C. Lavanchy, M. Polliand, D. Koerber, Dr. U. Kolitsch and Dr. C. Tenailleau. A special thank is also addressed to Dr. P.-J. Chiappero at the MNHN of Paris, for his help and for providing numerous crichtonite samples for study; Dr. N. Xanthopoulos (XPS measurements) and Dr. D. Baumann (IR spectroscopy) from EPFL in Lausanne. This research was mainly funded by the University of Lausanne and the Geological Museum of Lausanne (Switzerland).

References

Armbruster, T. & Kunz, M. (1990): Cation arrangement in a unusual uranium-rich senaite: crystal structure study at 130 K. *Eur. J. Mineral.*, **2**, 163-170.

Bancroft, G.M., Brown, J.R., Fyfe, W.S. (1979): Advances in, and application of, X-ray photoelectron spectroscopy (ESCA) in mineralogy and geochemistry. *Chem. Geol.*, **25**, 227-243.

Bannister, F.A. & Horne, J.E.T. (1950): A radioactive mineral from Mozambique related to davidite. *Mineral. Mag.*, **29**, 101-112.

Bermanec, V., Tibljas, D., Goran, K. (1990): Uranium-rich metamict senaite from Alinci, Yugoslavia. *Eur. J. Mineral.*, **4**, 331-335.

Damjanovic, A. & Vukasovic, M. (1961): A radioactive mineral from Crni Kamen in Macedonia – determined as davidite. *Radovi zavoda za nuklearne sirovine,* Beograd, **123**, 11-14. [in Serbo-Croatian]

De Bournon, J.L. (1817): Craitonite (*Nobis.*) & Observations additionnelles à la Craitonite. *in* Catalogue de la Collection Minéralogique particulière du Roi, ed. Imprimerie d'Abel Lanoë, Paris, 430-435, 468 & 417 pl. [in French]

Dragila, M. (1990): Observatli mineralogice asupra unul nou mineral din grupa daviditului. *Revista Minelor / Mine Petrol si Gaze,* Bucarest, **41**, 414-418. [in Romanian]

Finnie, K.S., Zhang, Z., Vance, E.R., Carter, M.L. (2003): Examination of U valence states in the brannerite structure by near-infrared diffuse reflectance and X-ray photoelectron spectroscopies. *J. Nucl. Mat.*, **317**, 46-53.

Fleischer, M. (1973): New Mineral Names: miromirite. *Am. Mineral.*, **58**, 560-562.

Foord, E.E., Sharp, W.N., Adams, J.W. (1984): Zinc- and Y-group-bearing senaite from St Peters Dome, and new data on senaite from Dattas, Minas Gerais, Brazil. *Mineral. Mag.*, **48**, 97-106.

Gatehouse, B.M., Grey, I.E., Campbell, I.H., Kelly, P.R. (1978): The crystal structure of loveringite – a new member of the crichtonite group. *Am. Mineral.*, **63**, 28-36.

Gatehouse, B.M., Grey, I.E., Kelly, P.R. (1979): The crystal structure of davidite. *Am. Mineral.*, **64**, 1010-1017.

Gatehouse, B.M., Grey, I.E., Smyth, J.R. (1983): Structure refinement of mathiasite, $(K_{0.62}\ Na_{0.14}\ Ba_{0.14}\ Sr_{0.10})_{\Sigma 1.0}\ [Ti_{12.90}\ Cr_{3.10}\ Mg_{1.53}\ Fe_{2.15}\ Zr_{0.67}\ Ca_{0.29}\ (V, Nb, Al)_{0.36}]_{\Sigma 21.0}\ O_{38}$. *Acta Cryst.*, **C39**, 421-422.

Graeser, S. & Guggenheim, R. (1990): Brannerite from Lengenbach (Switzerland). *Schweiz. Mineral. Petrogr. Mitt.*, **70**, 325-331.

Grey, I.E. & Gatehouse, B.M. (1978): The crystal structure of landauite, $Na\ Mn\ Zn_2\ (Ti, Fe)_6\ Ti_{12}\ O_{38}$. *Can. Mineral.*, **16**, 63-68.

Grey, I.E. & Lloyd, D.J. (1976): The crystal structure of senaite. *Acta Cryst.*, **B32**, 1509-1513.

Grey, I.E., Lloyd, D.J., White, J.S. (1976): The structure of crichtonite and its relationship to senaite. *Am. Mineral.*, **61**, 1203-1212.

Hayton, J.D. (1960): The constitution of davidite. *Econ. Geol.*, **55**, 1030-1038.

Hey, M.H., Embrey, P.G., Fejer, E.E. (1969): Crichtonite, a distinct species. *Mineral. Mag.*, **37**, 349-356.

Holland, T.J.B. & Redfern, S.A.T. (1997): Unit cell refinement from powder diffraction data: the use of regression diagnostics. *Mineral. Mag.*, **61**, 65-77.

Hunter, B.A. (1997): RIETICA, version 1.7.7, IUCr Powder diffraction.

Il'menev, E.S., Portnov, A.M., Bochkov, S.V., Vostrova, S.I. (1972): New type of Baumhauer twins in landauite crystals. *Soviet Phys. Dokl.*, **17**, 85-87.

Kelly, P.R., Campbell, I.H., Grey, I.E., Gatehouse, B.M. (1979): Additional data on loveringite (Ca, REE) (Ti, Fe, Cr)$_{21}$O$_{38}$ and moshite discredited. *Can. Mineral.*, **17**, 635-638.

Larsen, A.O. (1989): Senaite from a syenite pegmatite at Tvedalen in the southern part of the Oslo Region, Norway. *Norsk Geol. Tidsskr.*, **69**, 235-238.

Meixner, H. (1979): Ein Bericht über Davidit vom Lohningbruch, Rauris, Salzburg. *Karinthin*, **81**, 144-147. [in German]

Mossman, D.J. (1985): Davidite: a review of Canadian occurences, and report on a recent find at Kommes Lake, Saskatchewan. *Can. Mineral.*, **23**, 495-500.

Oberholzer, W.F., Graeser, S., Reusser, E. (1997): Senaite, a new occurrence in an Alpine fissure. *Schweiz. Mineral. Petrogr. Mitt.*, **77**, 233-236.

Orlandi, P., Pasero, M., Duchi, G., Olmi, F. (1997): Dessauite, (Sr,Pb)(Y,U)(Ti,Fe^{3+})$_{20}$O$_{38}$, a new mineral of the crichtonite group from Buca della Vena mine, Tuscany, Italy. *Am. Mineral.*, **82**, 807-811.

Orlandi, P., Pasero, M., Rotiroti, N., Olmi, F., Demartin, F., Moëlo, Y. (2004): Gramaccioliite-(Y), a new mineral of the crichtonite group from Stura Valley, Piedmont, Italy. *Eur. J. Mineral.*, **16**, 171-175.

Pabst, A. (1961): X-ray crystallography of davidite. *Am. Mineral.*, **46**, 700-718.

Portnov, A.M., Nikolayeva, L.Y., Stolyarova, T.I. (1966): A new titanium mineral, landauite. *Dokl. Akad. N. SSSR*, **166**, 1420-1421.

Rouse, R.C. & Peacor, D.R. (1968): The relationship between senaite, magnetoplumbite, and davidite. *Am. Mineral.*, **53**, 869-879.

Salje, E.K.H., Chrosch, J., Ewing, R.C. (1999): Is "metamictization" of zircon a phase transition? *Am. Mineral.*, **84**, 1107-1116.

Schaer, J.-P. (1959): Géologie de la partie septentrionale de l'éventail de Bagnes. *Arch. Sc.,* Geneva, **12**, 473-617. [in French]

Smellie, J.A.T., Cogger, N., Herrington, J. (1978): Standards for quantitative microprobe determination of uranium and thorium with additional information on the chemical formulae of davidite and euxenite-polycrase. *Chem. Geol.*, **22**, 1-10.

Stalder, H.A. & Bühler, C. (1987): Geochemische Untersuchungen an Mineralien der Crichtonit-Gruppe aus alpinen Zerrklüften. *Schweiz. Mineral. Petrogr. Mitt.*, **67**, 93-102. [in German]

Strunz, H. & Nickel, E.H. (2001): Strunz Mineralogical Tables. Chemical Structural Mineral Classification System. 9th Edition, E. Schweizerbart'sche Verlagsbuchhandlung (Nägele u. Obermiller), Stuttgart, 870 pp.

Thélin, P., Sartori, M., Burri, M., Gouffon, Y., Chessex, R. (1993): The pre-Alpine basement of the Briançonnais (Wallis, Switzerland). *in* Pre-Mezosoic Geology in the Alps, J. Von Raumer, ed. Springer Verlag, Berlin, 297-315.

Wang, D. (1981): Plumbodavidite – a new variety of davidite. *Chin. Sci. Bull.,* **26**, 915-919.

Williams, D.H. & Fleming, I. (1980): Spectroscopic Methods in Organic Chemistry. 3rd Ed., McGraw-Hill, London, 251 pp.

Wilson, A. (1960): The microdetermination of ferrous iron in silicate minerals by a volumetric and colorimetric method. *Analyst*, **85**, 823-827.

Wülser, P.-A. (1996): Prospection alluvionnaire pour la scheelite et recherche de l'uranium dans la région de Cleuson (Val de Nendaz, Suisse). 30. Wettbewerb, Lausanne. Schweizer Jugend Forscht, 37. [in French]

– (2002): Métarhyolites et métasediments de la Nappe du Mont Fort (Valais, Suisse) & Minéraux du groupe des crichtonites: présentation d'une nouvelle espèce. Diploma Work, Université de Lausanne, Lausanne, 225 p. [in French]

Zhang, J., Ma, J., Li, L. (1988): The crystal structure and crystal chemistry of the lindsleyite and mathiasite. *Geol. Rev.*, **34**, 132-144. [in Chinese]

Received 25 August 2004
Modified version received 25 February 2005
Accepted 30 May 2005